SUBMITTED

CHAPTER X

Multimodal targeted high relaxivity thermosensitive liposome for in vivo imaging

Maayke M P Kuijten[1,4,5], M. Hannah Degeling[1,4,6], John W. Chen[2,3], Gregory Wojtkiewicz[3], Peter Waterman[3], Ralph Weissleder[3], Klaas Nicolay[5] and Bakhos A Tannous[1,4].

[1]Neuroscience Center and Molecular Neurogenetics Unit, Department of Neurology, [2]Division of Neuroradiology, Department of Radiology, [3]Center for Systems Biology, Massachusetts General Hospital, and [4]Program in Neuroscience, Harvard Medical School, Boston, MA 02114 USA. [5]Department of Biomedical Engineering, Biomedical NMR, Eindhoven University of Technology, Eindhoven, the Netherlands. [6]Department of Neurosurgery, Leiden University Medical Center, Leiden, the Netherlands.

ABSTRACT

Liposomes are spherical, self-closed structures formed by lipid bilayers that can encapsulate drugs and/or imaging agents in their hydrophilic core or within their membrane moiety, making them suitable delivery vehicles. We have synthesized and characterized a new targeting, thermosensitive liposome, containing gadolinium-DOTA lipid bilayer, as a multimodal molecular imaging agent for magnetic resonance and optical imaging. We showed that this liposome has a much higher molar relaxivities r1 and r2 compared to a more conventional liposome containing gadolinium-DTPA-BSA lipid. By incorporating both gadolinium and rhodamine in the lipid bilayer as well as biotin on its surface, we used this agent for multimodal imaging and targeting of tumors through the strong biotin-streptavidin interaction. Since this new liposome is thermosensitive, it can be used for ultrasound-mediated drug delivery at specific sites, such as tumors, and can be guided by magnetic resonance imaging.

INTRODUCTION

Magnetic resonance imaging (MRI) is a routine diagnostic tool with many advantages compared to other imaging modalities including its noninvasive character, lack of radiation burden and its excellent spatial and temporal resolution[1, 2]. Despite its many advantages, there are intrinsic limitations caused by MRI contrast agents, such as short vascular half-life circulation, which could lead to potential side effects. This drawback can be overcome by using liposomes which can incorporate a high payload of gadolinium-containing amphiphilic lipid in their bilayer resulting in a spectacular increase in effective longitudinal (r1) relaxivity per particle[3-5].

Liposomes are spherical, self-closed structures formed by one or more lipid bilayers and contain an aqueous phase inside and between bilayers[6]. The amphiphilic lipids used for the formation of liposomes are usually comprised of a hydrophilic head group and two hydrophobic fatty acyl chains. Their amphiphilic character results in spontaneous assembly into aggregates in aqueous environment. Hydrophilic drugs can be enclosed in the aqueous compartment while hydrophobic

drugs can be incorporated in the lipid bilayers core[7, 8]. These characteristics together with their potential to invade the immune system, target cells, and reduce unwanted side-effects made them the drug delivery vehicle of choice[3, 4, 6, 9]. Further, the surface of liposomes can be modified and grafted with different targeting moieties including antibodies or bioresponsive components like biosensitive lipids or polymers[8]. In addition to drug delivery, the success of liposomes has led to their use as carriers for imaging agents since they can either encapsulate a contrast agent, a fluorophore for optical imaging, or both within their interior or in their bilayer. This characteristic overcomes problems associated with these imaging agents such as rapid clearance, non-specific cellular interaction, and toxicity resulting in poor contrast and low resolution images[3, 8].

Multifunctional liposomes have been developed for image-guided drug delivery by incorporating both therapeutic drugs and contrast agents for MRI[3, 4]. Typically, lipid-based contrast agents such as amphiphilic gadolinium(Gd)-DTPA derivatives are incorporated within the membrane moiety of the liposome, leaving the lumen to encapsulate therapeutic molecules[2, 10]. The disadvantage of these liposomes is that they contain a single Gd-chelate moiety per molecule leading to lower MRI detectability. In an attempt to overcome these limitations, macromolecular Gd-chelates with several residues in the single molecular chain have been used, however, these polychelates could change the liposome structure, affecting its surface properties[2, 11]. Thermosensitive liposomes have been developed for ultrasound-mediated drug delivery at specific sites, such as tumors [12-14], and can be guided by imaging[10, 15, 16]. These liposomes typically incorporates the contrast agent within their lumen for which relaxivity is low when the liposome is intact and only increases during phase transition[17].

Given these limitations, an alternative strategy to enhance detectability with MRI is to increase the effective longitudinal relaxivity per Gd-chelate moiety. In this study, we synthesized and characterized a new liposome, named NLP, which contains Gd-DOTA lipid bilayer and is thermosensitive due to the addition of lipids with transition temperatures below 45 °C. We compared the activity of this liposome to a more conventional liposome (CLP; with a transition temperature of 60 °C) containing Gd-DTPA-BSA lipid and showed that NLP has a much higher efficacy as

a MRI contrast agent. By embedding the gadolinium imaging agent in the membrane of the liposome, this agent exhibits high intrinsic relaxivity when the liposome is intact, making it suitable for monitoring the delivery of drug carriers to the target. Further, we engineered a targeting multifunctional liposome based on NLP which carries both gadolinium and a fluorophore in the lipid bilayer as well as biotin on its surface, and demonstrated that it could be used for multimodal molecular imaging and targeting of tumors through the strong biotin-streptavidin interaction.

RESULTS

Synthesis and characterization of the NLP liposome formulation. We have synthesized a thermosensitive liposome with gadolinium containing lipids as a new contrast agent for MRI (**Fig. 1**). We compared the characteristics of this new formulation (NLP) to a more conventional DSPC-based Gd-containing liposome (CLP, **Fig. 1**). We first measured the mean average hydrodynamic diameter of the NLP liposome and showed it to be 86 nm, which is smaller than the conventional CLP liposome having a size of 109 nm (**Fig. 2a** and **Table 1**). The mean average diameter of the NLP liposome, stored at 4 ºC, was again investigated after 5 weeks. We observed that both the size and size distribution of the liposome remained constant with an average hydrodynamic diameter of 85 nm (data not shown). The consistency of these results indicates a sterically-stabilized liposome preparation with a shelf lifetime of at least 5 weeks.

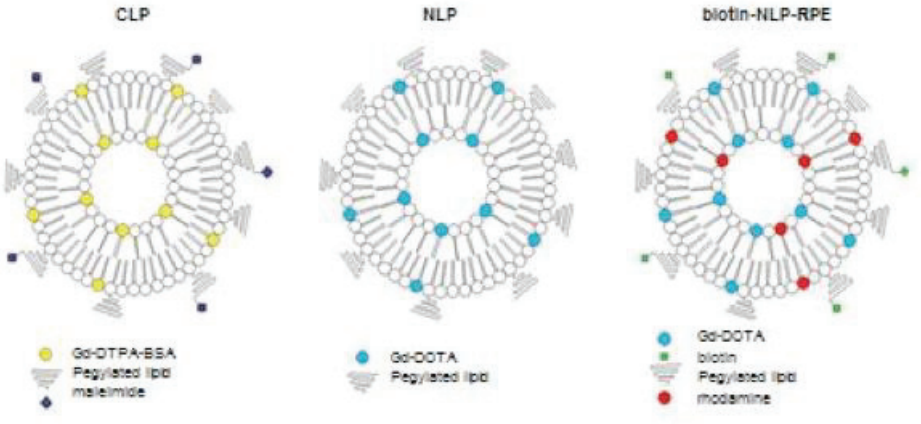

Figure 1. Schematic overview of CLP, NLP and NLP-biotin-RPE liposomes.
We synthesized a new DPPC-based liposome (NLP) containing gadolinium-DOTA lipid and compared its characteristics to more conventional DSPC-based liposome with gadolinium-DTPA-BSA (CLP). In order to make NLP multifunctional, a biotin and rhodamine containing lipid was added to the formulation so the liposome can be traced both with magnetic resonance and fluorescence imaging and can be targeted using the strong biotin-streptavidin interaction (NLP-biotin-RPE).

In order to determine the efficacy of the different liposomes as contrast agents, we determined the gadolinium ion concentration in both NLP and CLP. The Gd(III) concentration estimated by phosphate determination for CLP and NLP was 2.790 mM and 1.925 mM respectively (**Table 1**). The Gd(III) concentration in the these liposome were also precisely determined using inductively coupled plasma mass spectroscopy (ICP-MS) and found to be 2.920 mM and 2.238 mM, respectively, similar to the concentration found by phosphate determination (**Table 1**).

Table 1: Characterization CLP, NLP and biotin-NLP-RPE liposomes.

Characteristics	CLP	NLP	biotin-NLP-RPE
Size	109 nm	86 nm	93 nm
Concentration Gd(III) by phosphate determination	2.8 mM	1.9 mM	1.8 mM
Concentration Gd(III) by ICP	2.9 mM	2.2 mM	1.9 mM

Thermosensitivity of NLP liposome. To determine the thermosensitivity of the NLP liposome, calcein release during heating was investigated. The fluorescent signal of calcein is quenched due to its high concentration (30 mM) inside the aqueous lumen of the liposome. During phase transition, the lipids in the liposome rearrange and the liposome shell opens resulting in calcein release and hence increased fluorescence signal. Upon liposome heating, lipid rearrangement started at 38 °C resulting in leakage of its content (**Fig. 2b**).

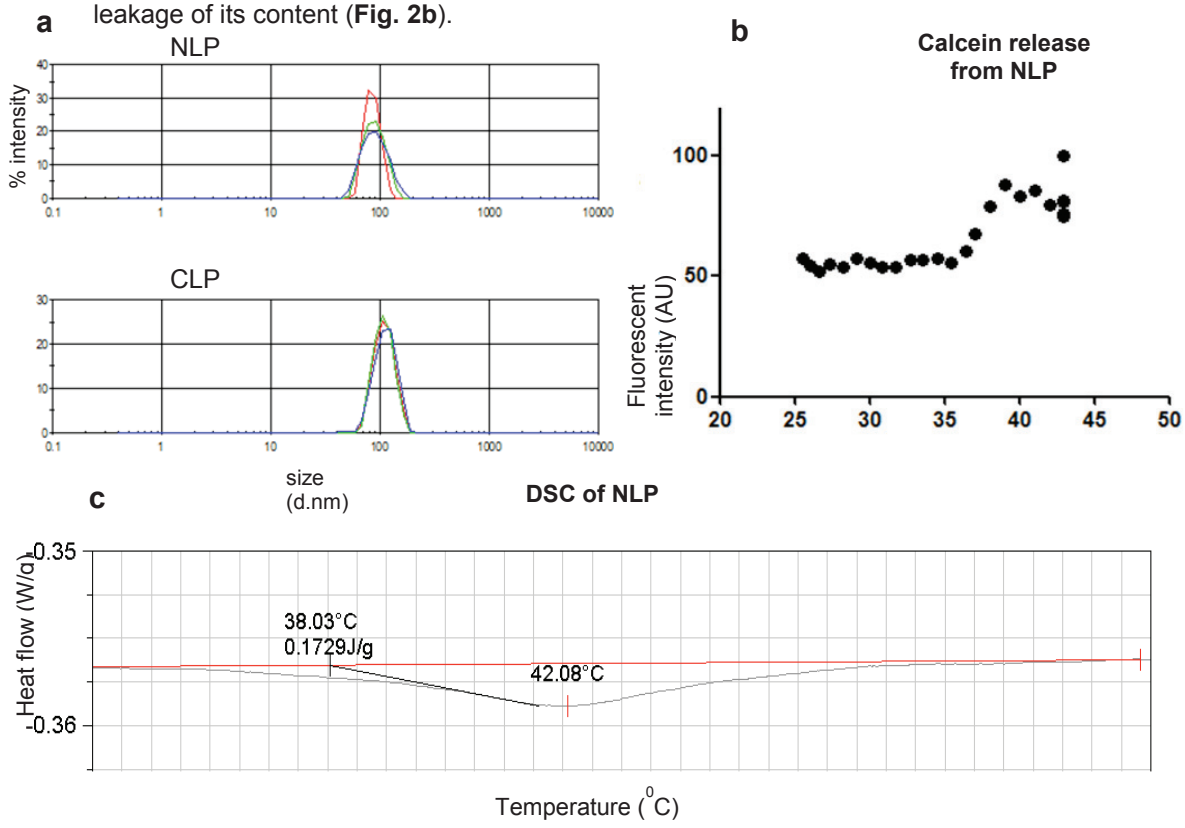

Figure 2. Size distribution and thermosensitivity of NLP and CLP liposomes. (a) The size of the liposome was measured with dynamic light scattering. Intensity plots showing the average hydrodynamic diameters of NLP and CLP to be 86 nm and 109 nm respectively. (b) NLP-containing calcein was heated at different temperatures. The fluorescent intensity starts to increases around 37 - 38 ºC indicating lipid rearrangement and further increases until around 39 ºC. No significant further increase is visible upon addition of the lysis reagent triton X-100. (c) Differential scanning calorimetry (DSC) showing that NLP has a transition temperature of 42 ºC.

The fluorescent signal further increased until around 39 ºC at which temperature all calcein appeared to be released. No further increase in fluorescence signal was visible upon the addition of the lysis reagent Triton X-100, showing that all calcein was already released during the 40 minutes heating period. The transition temperature of NLP defined as the temperature at the top of transition phase was determined with differential scanning calorimetry (DSC) and found to be 42 ºC (**Fig. 2c**).

Relaxivity determination of NLP liposome. The measured Gd(III) concentration was used to determine the longitudinal (r1) and the transversal (r2) relaxivities of the different liposome formulations. Since NLP is thermosensitive (due to the incorporation of the DPPC and DMPC lipids), r1 and r2 relaxivities were determined at different temperatures to investigate the influence of hyperthermia on the imaging efficacy of this liposome. Longitudinal and transversal relaxivities of the liposome formulations at different temperatures were obtained from the slope of the linear fit of relaxation rates as a function of Gd(III) concentration. At higher temperature, both r1 and r2 relaxivities of the NLP decreased showing a negative influence of hyperthermia on imaging efficacy of NLP (**Fig. 3a**).

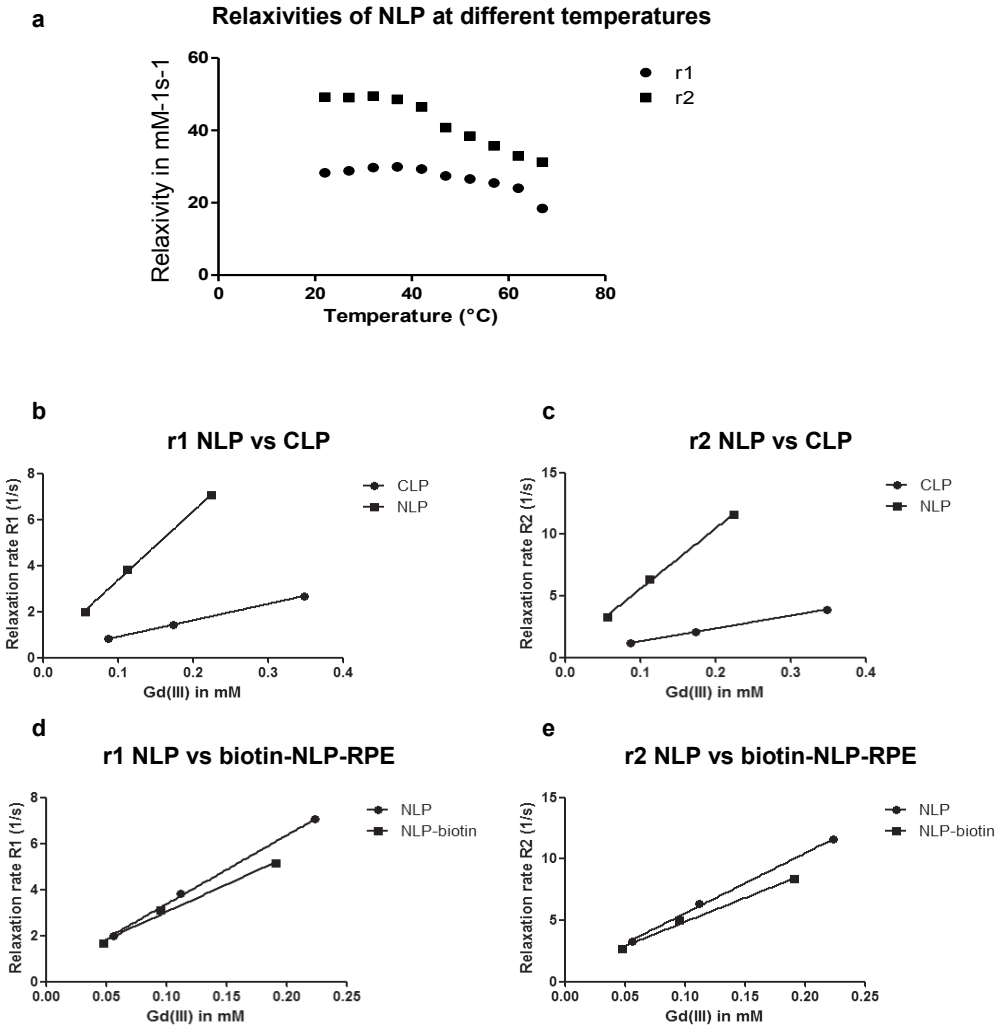

Figure 3. Longitudinal and transversal relaxivities of the different liposome formulations in $mM^{-1}s^{-1}$. Longitudinal (r1) and transversal (r2) relaxivities were obtained from NMR measurements at 60 MHz and 1.41 Tesla. **(a)** longitudinal and transversal relaxivities of NLP liposomes obtained at different temperatures ranging from 22 °C to 67 °C with 5 °C intervals. **(b,c)** Longitudinal and transversal relaxation rates of NLP as compared to CLP liposomes obtained at 37 °C. **(d,e)** Relaxation rates of NLP versus NLP-biotin-RPE are presented.

To determine the efficacy of NLP as a contrast agent, r1 and r2 relaxivities at 37 °C were compared to the conventional CLP liposome. T1 and T2 measurements were performed at 60 MHz corresponding to a magnetic field strength of 1.41 Tesla.

The Gd(III)DTPA-BSA-based CLP liposome exhibited a longitudinal r1 relaxivity of 7.52 $mM^{-1}s^{-1}$ (**Table 2, Fig. 3b**), which is similar to values published for the same formulation (7.5 $mM^{-1}s^{-1}$)[18]. The transversal r2 relaxivity of CLP was found to be 10.6 $mM^{-1}s^{-}1$. On the other hand, the Gd(III)DOTA-DSPE based NLP liposome exhibited four-fold higher r1 of 29.9 $mM^{-1}s^{-1}$ and five-fold higher r2 of 49.0 $mM^{-1}s^{-1}$ as compared to CLP (**Table 2, Fig. 3b,c**). The longitudinal relaxivity of NLP was >2-fold higher compared to the published relaxivity for DSPC-based Gd(III)DOTA-DSPE containing liposome (12.8 $mM^{-1}s^{-1}$)[18]. The reported relaxivities are the average relaxivities of the Gd(III) ions in the inner and outer leaflets of the lipid bilayer.

Table 2: Longitudinal (r1) and transversal (r2) relaxivities in $mM^{-1}s^{-1}$ of CLP, NLP and biotin-NLP-RPE liposome formulations at 37°C obtained from NMR measurements at 60 MHz at 1.5 Tesla.

Relaxivity at 37° C	CLP	NLP	Biotin-NLP-RPE
Relaxivity r1	7.5 $mM^{-1}s^{-1}$	29.9 $mM^{-1}s^{-1}$	23.9 $mM^{-1}s^{-1}$
Relaxivity r2	10.6 $mM^{-1}s^{-1}$	49.0 $mM^{-1}s^{-1}$	39.0 $mM^{-1}s^{-1}$
r2/r1	1.41	1.64	1.64

Synthesis and characterization of a targeted multimodal NLP liposome. In order to increase sensitivity and selectivity of the newly formulated contrast agent, targeted NLP was synthesized with a biotin on its surface (biotin-NLP). Further, to make NLP suited for multimodal imaging (fluorescence and MRI), rhodamine-PE (RPE) was added within the lipid bilayers of the liposome (biotin-NLP-RPE; **Fig. 1**). The addition of biotin and rhodamine to the NLP formulation did not affect its size (93 nm, **Table 1**). The gadolinium ion concentration as well as the longitudinal, and transversal relaxivities of biotin-NLP-RPE were found to be similar to the non-targeted NLP liposome (**Table 1,2; Fig. 3d,e**).

Targeting of cells with biotin-NLP-RPE in culture. To determine the functionality of the newly synthesized biotin-NLP-RPE liposome in targeting tumor cells, viable Gli36 human glioma cells overexpressing both the mutant EGFRvIII, a frequent genetic alteration in primary brain tumors[19] and GFP, or plain Gli36 control cells were incubated with a biotinylated antibody against EGFRvIII followed by Streptavidin-Alexa647 and finally by biotin-NLP-RPE and analyzed by fluorescence microscopy.

A distinct surface staining of both Alexa647 (indicative of streptavidin binding) and rhodamine-PE (liposome) was observed, showing the functionality of this liposome in targeting tumor cells (**Fig. 4a**). The plain Gli36 cells did not show any surface staining (data not shown).

To evaluate the usefulness of the biotin-NLP-RPE in targeting tumor cells in a different model, Gli36 human glioma cells were engineered by a lentivirus vector to express both GFP (marker for transduction efficiency) as well as a fusion protein between a biotin acceptor peptide (BAP), preceded by a signal sequence, and the transmembrane domain (TM) of the PDGFR receptor (BAP-TM)[20]. Upon gene transfer and expression, the biotin ligase will tag the BAP peptide with a single biotin moiety which is presented on the cell surface through TM. These cells as well as control cells were then labeled with streptavidin-Alexa647 followed by incubation with biotin-NLP-RPE and analyzed by fluorescence microscopy. A distinct cell surface staining was found on cells expressing BAP-TM for both Alexa647 and RPE proving the specific targeting of biotin-NLP-RPE (**Fig. 4b**). Control cells did not show any surface staining (data not shown).

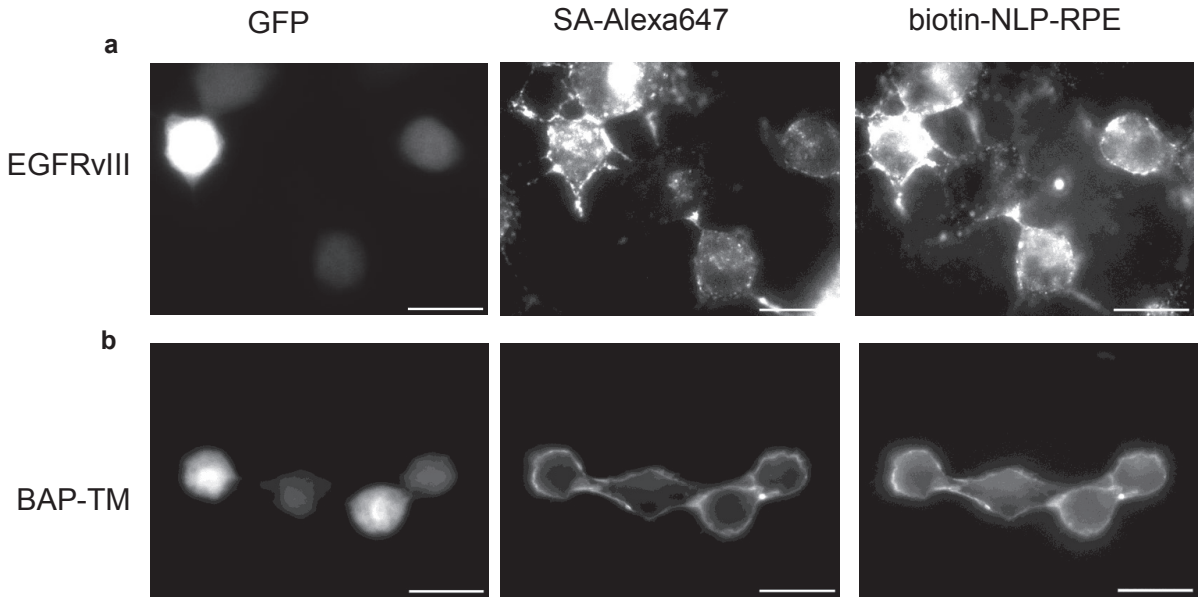

Figure 4. Targeting of cells with biotin-NLP-RPE liposome. (**a**) Gli36 human glioma cells expressing the EGFRvIII receptor and GFP were labeled with a biotinylated-antibody against EGFRvIII followed by streaptavidin-Alexa647 and biotin-NLP-RPE, and analyzed by fluorescence microscopy for both Alexa647 and RPE. (**b**) Gli36 cells were infected with

lentivirus vector expressing BAP-TM and GFP. These cells were labeled with Streptavidin-Alexa647 followed by biotin-NLP-RPE and analyzed as in (a).

Targeted multimodal *in vivo* imaging of tumors using biotin-NLP-RPE. To confirm the functionality of biotin-NLP-RPE in an *in vivo* model, Gli36 cells engineered by gene transfer to express BAP-TM or plain Gli36 control cells were injected subcutaneously in the flanks of nude mice (n=5) at two different locations. Two-weeks later, mice were i.v. injected with either biotin-NLP-RPE or a complex consisting of biotin-NLP-RPE and streptavidin-Alexa750 (Alexa750-SA-NLP-RPE) and imaged first with fluorescence-mediated tomography (FMT; 4 hrs post-injection) for Alexa750 confirming streptavidin targeting. Significant accumulation (*$p<0.001$) of Alexa750 signal was observed in tumors expressing biotin on their surfaces as compared to control tumors in mice injected with Alexa750-SA-NLP-RPE and not the non-targeted biotin-NLP-RPE (without the use of streptavidin), showing efficient targeting of this NLP complex to biotin expressing tumors (**Fig. 5a,b**). The same mice were also imaged with T1w MRI at 4 and 24 hrs post-injection. Significantly higher accumulation (*$p<0.001$) of NLP liposome over time was observed in tumors expressing biotin on their surfaces as compared to control tumors only in mice injected with targeted Alexa750-SA-NLP-RPE complex showing that tumors can be targeted and imaged with MR using this liposome complex (**Fig. 5c,d**). Mice injected with non-targeted biotin-NLP-RPE liposome showed similar and lower accumulation in both tumors.

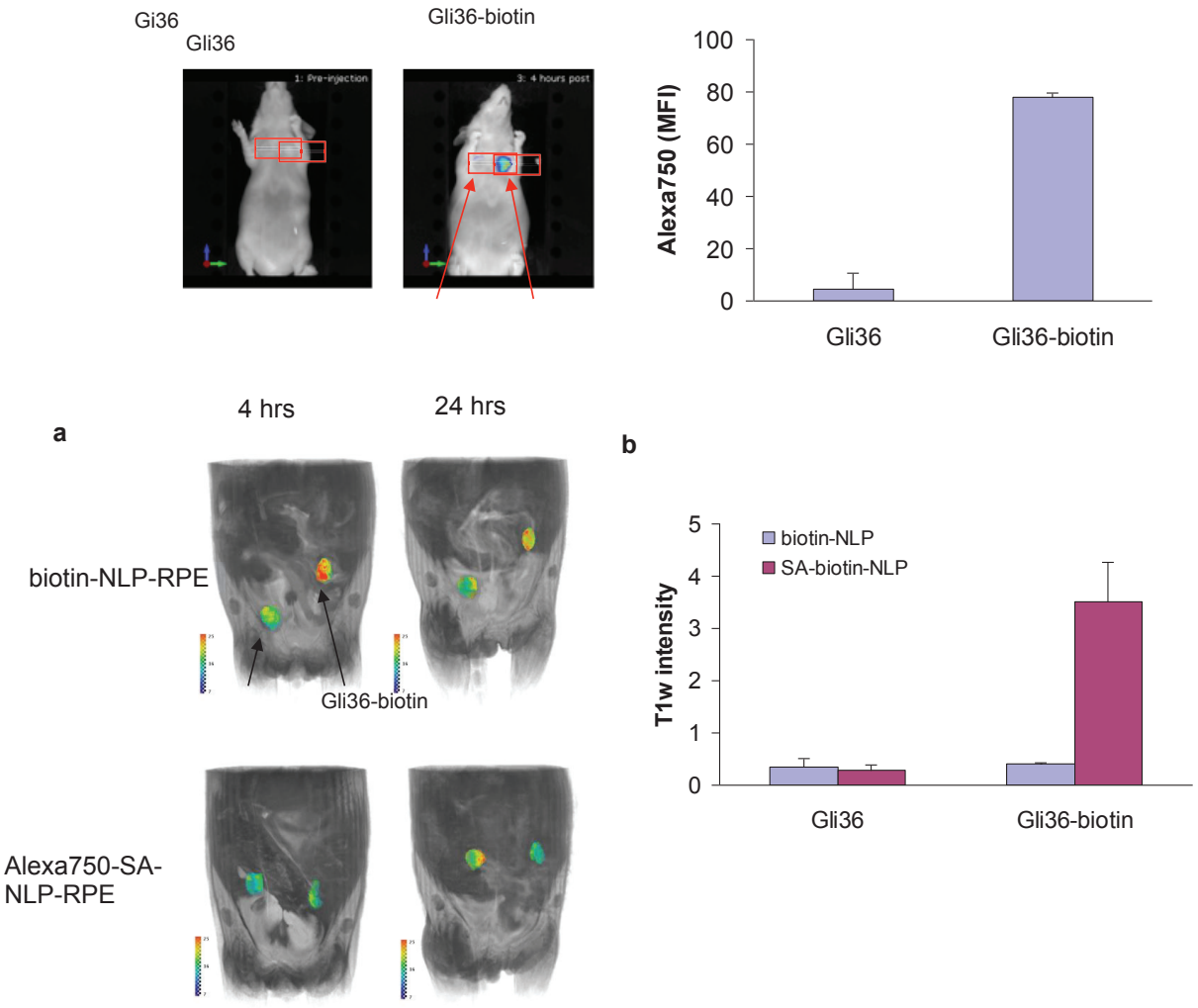

Figure 5. Targeting and in vivo imaging of tumors with biotin-NLP-RPE. Gli36 human glioma cells or same cells expressing biotin on their surfaces (through BAP-TM) were implanted subcutaneously in nude mice (n=5) at 2 different sites. Two-weeks later, mice were i.v. injected with either biotin-NLP-RPE or a complex consisting of biotin-NLP-RPE and streptavidin-Alexa750 (Alexa750-SA-NLP-RPE) and imaged 4 hrs later with FMT Alexa750. (**a-b**) a representative mouse from each group is shown in (a) and quantitation of fluorescent accumulation in each tumor in (b). (**c-d**) The same mice were also imaged with T1w MRI at 4 and 24 hrs post-injection (c). T1w intensities at 24 hrs were normalized to 4 hrs for each tumor (d). *p<0.001 as calculated by student's t-test.

DISCUSSION

In this study, we synthesized a new liposome and characterized it by comparing its efficacy as a contrast agent to a more conventional liposome. We showed that the new liposome NLP exhibited four-fold higher longitudinal and five-fold higher transversal relaxivity compared to a conventional liposome CLP. Further, the longitudinal relaxivity (at 1.41 Tesla) of NLP was >2-fold higher compared to a published liposome formulation with the same Gd-DOTA containing lipid (29.9 $mM^{-1}s^{-1}$ compared to 12.8 $mM^{-1}s^{-1}$)[18]. Since the NLP formulation is thermosensitive, we observed a temperature dependency for both longitudinal and transversal relaxivities being lower at higher temperature. Recent studies showed that an increase in temperature leads to an increase in longitudinal relaxivity for DSPC-based Gd(III)DOTA-DSPE containing liposomes (12.8 $mM^{-1}s^{-1}$ at 37°C compared to over 14 $mM^{-1}s^{-1}$ at 67 °C)[18]. A potential explanation for these differences between typical liposomes and NLP could be the increased water exchange across the liposomal membrane at higher temperature resulting in larger contribution of Gd(III)DOTA-DSPE in the inner leaflet of the liposome to the overall longitudinal relaxivity[21-24]. The unique composition of the NLP liposome could possibly positively affect the water exchange across the liposomal membrane and explain its high relaxivities compared to both CLP and Gd(III)DOTA-DSPE containing liposome. To further increase the sensitivity and selectivity of the NLP contrast agent, and to make it useful for multimodal imaging, we synthesized the NLP liposome with biotin on its surface and rhodamine within the lipid bilayer. The Gd(III) inside the liposome can serve as a contrast agent for MRI and the rhodamine can be used for imaging at the single cell level with fluorescence. This biotin-NLP-RPE showed to have three to four-fold higher relaxivities compared to CLP[18]. Further, we showed that streptavidin can serve as a bridge between biotin-NLP-RPE and biotinylated antibody to target specific receptors overexpressed on tumor cells.

In vivo optical imaging has limited use due to the problem of light absorption by pigmented molecules such as hemoglobin and scattering by mammalian tissues, leading to a decrease in the detection limit. The biotin-NLP-RPE was synthesized with a rhodamine-containing lipid in the bilayer, which was shown to be useful in targeting tumor cells at the single cell level in culture using fluorescence imaging. This same complex would be useful for single cell detection in vivo using intravital

micoscopy and could be extended for intraoperative fluorescence imaging[25]. Further, the rhodamine can be replaced with any fluorophore emitting in the near infra-red region of the spectrum, which can then be used for FMT imaging in deep tissues *in vivo*[26]. The biotin on the NLP surface makes these liposomes universal targeted contrast agents for which practically any peptide/antibody specific to a cell of interest can be complexed to it through the strong interaction of biotin with streptavidin. The specificity of biotin to streptavidin has been exploited for several medical and scientific applications including drug or toxin targeting, *in vivo* imaging of targeted cells, and antibody-guided radioimmunotherapy in humans[20, 27, 28].

The use of biotin-NLP-RPE liposome can be extended and applied for drug delivery. The combination of imaging with drug delivery is very valuable in the search for new therapeutic strategies. Further, the thermosensitive characteristic of this liposome does not only have a positive effect on the relaxivity, but could also be used as a delivery strategy for drugs, for instance to solid tumors. Our *in vitro* data shows that a temperature of 39 ^{0}C can lead to an increase in calcein release from NLP liposomes. This thermosensitive feature of NLP has a high clinical impact in which NLP liposome can encapsulate a therapeutic drug which can be released specifically on the tumor site by ultrasound-induced hyperthermia, similar to previously published methods [10, 15, 16]. Further, by including Gd(III) in these liposomes, MRI can be used for guided drug release at the specific site[10].

In conclusion, we have synthesized a new liposome with higher r1 and r2 relaxivities as compared to conventional liposome and showed it to be useful for targeting and multimodal imaging of tumors. Since this liposome is thermosensitive, it can be used for ultrasound-mediated drug delivery at specific sites, such as tumors, which can be guided by MRI or catheter based optical imaging [29-32]

MATERIALS AND METHODS

Materials for liposome preparation. 1,2-Dipalmitoyl-sn-glycero-3-phosphocholine (DPPC), 1,2-ditetradecanoyl-*sn*-glycero-3-phosphocholine (DMPC), 1,2-distearoyl-sn-glycero-3-phosphoethanolamine-N-[methoxy(polyethylene glycol)-2000] (PEG2000-DSPE), 1,2-distearoyl-sn-glycero-3-phosphoethanolamine-N-[biotinyl(polyethylene glycol)2000] (Biotin-PEG2000-DSPE), 1,2-Dioleoyl-sn-Glycero-

3-Phosphoethanolamine-N-(Lissamine Rhodamine B Sulfonyl) (Rhodamine PE), 1,2-distearoyl-sn-glycero-3-phosphoethanolamine-N-[maleimide(polyethylene glycol)-2000] (PEG2000-DSPEmal), 1,2-Distearoyl-sn-glycero-3-phosphocholine (DSPC) and cholesterol were purchased from Avanti Polar Lipids (Alabaster, AL). Gd(III)DOTA-DSPE and Gd(III)-DTPA-bis(stearylamide) (Gd(III)-DTPA-BSA) were obtained from Gateway Chemical Technology (St. Louis, MO).

Preparation of liposome formulations. Liposomes were prepared according to three different formulations: the more conventional liposome DSPC-Gd(III)DTPA-BSA (CLP), the new formulation DPPC-Gd(III)DOTA (NLP) and the new formulation biotinylated and rhodamine-labeled: DPPC-Gd(III)DOTA-biotin (biotin-NLP-RPE). NLP liposome was prepared with DPPC, DMPC, Gd(III)DOTA-DSPE and PEG2000-DSPE at a molar ratio of 50:20:25:5 (**Table 3**). As a control, CLP liposome were used containing DSPC, Gd(III)DTPA-BSA, PEG2000-DSPE, PEG 2000-DSPEmal and cholesterol in a molar ratio of 36.7: 25:2.5:2.5:33.3 (**Table 3**). The biotin-NLP-RPE liposome was prepared with DPPC, DMPC, Gd (III)DOTA-DSPE, PEG2000-DSPE, Biotin-PEG2000-DSPE and Rhodamine PE at a molar ratio of 50:20:25:2.5:2.5:0.1 (**Table 3**). These liposomes were prepared by lipid film hydration followed by extrusion[5]. The lipid film was prepared by dissolving the lipid mixture (50 µmol) in 3:1 v/v $CHCl_3$/MeOH in a 250 ml round-bottomed flask. The solution was evaporated using rotation evaporation for 15 minutes at 200 mbar and 30 ºC and at 150 mbar till dryness. In order to assure complete dryness, rotation evaporation was pursued at 0 mbar for 15 more minutes and the film was subsequently put under a nitrogen flow for at least one hour. The NLP and biotin-NLP-RPE films were dried over night. The films were hydrated with 4 ml HEPES buffered saline (HBS) (20 mM HEPES and 135 mM NaCl at pH 7.4) at 60 ºC for NLP and biotin-NLP-RPE and 65 ºC for the CLP liposomes after heating the film to 65 ºC. The films of the NLP and biotin-NLP-RPE liposomes were not heated before addition of the HBS. The lipid dispersions were extruded (Lipofast Extruder, Avestin, Ottawa, Ontario) at 60 ºC and 65 ºC for the NLP and CLP liposomes respectively. The lipid dispersions were extruded through polycarbonate membrane filters (Whatman, Maidstone, UK) with a pore diameter of 400 nm (1 time), through filters with a pore diameter of 200 nm (6 times) and through filters with a pore diameter of 100 nm (6 times).

Table 3. Formulations of CLP, NLP and biotin-NLP-RPE liposomes.

CLP	Mol %	NLP	Mol %	NLP-biotin-RPE	Mol %
DSPC	36.67	DPPC	50	DPPC	50
Gd(III)DTPA-BSA	25	DMPC	20	DMPC	20
Cholesterol	33.33	Gd(III)-DOTA-DSPE	25	Gd(III)-DOTA-DSPE	25
PEG2000-DSPE	2.5	PEG2000-DSPE	5	PEG2000-DSPE	2.5
PEG2000-DSPEmal	2.5			Biotin-PEG2000-DSPE	2.5
				Rhodamine PE	0.1

Liposome characterization. The size and size distribution of liposomes were measured using dynamic light scattering (DLS) at 25, 37 or 41 °C on a Malvern Zetasizer Nano S apparatus (Malvern, UK) equipped with a 633 nm laser. These measurements were performed in sextuple using three different concentrations of liposome suspension in 400 µl HBS (20 mM HEPES and 135 mM NaCl at pH 7.4).

Total lipid and gadolinium [Gd(III)] concentrations of liposome suspensions were calculated using phosphate determination, performed according to Rouser after destruction of the samples with perchloric acid at 180 ºC[33]. The amount of phospholipids in the sample was determined using a calibration curve between 0 and 80 nmol phosphate. The total amount of lipids and the amount of gadolinium containing lipids in the sample was calculated based on the measured amount of phospholipids.

The gadolinium ion concentration was determined for NLP and biotin-NLP-RPE liposomes using inductively coupled plasma mass spectroscopy (ICP-MS;

DRCII Perkin-Elmer, Philips Research Material Analysis, Eindhoven, The Netherlands). From each sample, 150 µl was taken, weighed and sent in for ICP.

Determination of thermosensitivity

The thermosensitivity of NLP liposome was determined based on calcein release experiment and differential scanning calorimetry. In order to measure calcein release, NLP liposome films (25 µmol) were hydrated with 2 ml of 30 mM calcein 100 mM NaCl solution in HBS (pH 6.8). Extrusion was performed according to the same protocol as for the NLP liposome. Free calcein was separated from calcein-containing liposome using PD-10 column (GE-healthcare). Liposome was then dissolved in HBS (20 mM HEPES and 135 mM NaCl; pH 7.4). The fluorescent intensity of the calcein-containing liposome was measured with a fluorometer (excitation wavelength: 494 nm; emission wavelength: 517 nm). As a control, the fluorescent intensity of the liposome was measured at room temperature before and after addition of 10% triton-X in water. The fluorescent intensity was measured every minute for 40 minutes. The first measurement was performed at 25 ºC and the temperature of the water bath increased by 1 ºC every minute. The temperature of the sample was measured every two minutes. After 40 minutes, 10% triton-X in water was added to the sample to determine the maximal fluorescent intensity. The phase transition temperature of NLP liposome was measured with differential scanning calorimetry (DSC, Universal V4 5A TA Instruments).

Determination of relaxivity. To determine the longitudinal and transversal relaxivities of the liposomes, spin-lattice relaxation time (T1) and spin-spin relaxation time (T2) measurements were performed on a Bruker (Rheinstetten, Germany) Minispec mq60 NMR analyzer (60 MHz) with a magnetic field of 1.41 Tesla. T1 relaxation times were obtained using the standard inversion recovery method with a recycle delay of 20 s, inversion time ranging from 5 ms to 10 seconds, the inversion sequence was repeated ten times and four averages. T2 times were measured using a Carr-Purcell-Meiboom-Gill (CPMG) sequence with a recycle delay of 20 s, interecho time of 0.4 ms, 10,000 echoes and 16 averages.

The longitudinal r1 and the transversal r2 relaxivities were obtained from the slope of the linear fit of relaxation rates as a function of gadolinium ion concentration described in equation 1 and 2 respectively (below). The relaxation rates R1 and R2

are the inverse of T1 and T2 respectively. The longitudinal and transversal relaxivities are a measure for the efficacy of the contrast agent.

$$\frac{1}{T1} = \frac{1}{T1_{tissue}} + r1[CA] \quad (1) \qquad \frac{1}{T2} = \frac{1}{T2_{tissue}} + r2[CA] \quad (2)$$

[CA] is the concentration of the contrast agent, in this case the Gd(III) concentration in mM and r1 and r2 the longitudinal and transversal relaxivity respectively[34]. In order to determine the relaxivities of the CLP, NLP and biotin-NLP-RPE liposomes, T1 and T2 measurements were performed at 37°C. Since NLP liposome is thermosensitive, relaxivities were determined at different temperatures. T1 and T2 measurements were performed within a temperature range of 22 °C to 67 °C with 5 °C intervals.

Cell culture. Gli36 human glioma cells were obtained from Dr. Anthony Capanogni, UCLA, CA. Gli36 cells were transduced with a retrovirus vector expressing the mutant EGFRvIII and puromycin resistant gene (obtained from Dr. Miguel Sena-Esteves, Department of Neurology, University of Massachusetts Medical Center, Worcester). The cells were selected by culturing the cells in conditioned media with 1 mg/l puromycin. Gli36 cells were also infected with a lentivirus vector expressing a biotin acceptor peptide, preceded by a signal sequence followed by the transmembrane domain of PDGFR (BAP-TM) as previously described[20]. As a control, Gli36 cells were infected with similar empty lentivirus vector. All cells were cultured in Dulbecco's modified Eagle's medium (DMEM) supplemented with 10% fetal bovine serum (Sigma, St. Louis, MO) and 100 U penicillin and 0.1 mg streptomycin (Sigma) per milliliter at 37 °C in a 5% CO_2 humidified incubator.

In vitro targeting of glioma cells with biotin-NLP-RPE. Seventy five thousand cells were plated in 1.5 ml conditioned media on coverslips (Fisher Scientific) in a 24 well plate. Twenty-four hours later, cells were incubated with 250 ng/ml of biotinylated anti-EGFRvIII antibody for 5 min (in phosphate buffer saline, PBS, a kind gift from Dr. Darell D. Bigner, Duke University Medical Center) at room temperature. Cells were then washed and incubated with streptavidin-Alexa647 (1:200; Molecular Probes) for 5 min. Cells were washed again and incubated with biotin-NLP-RPE (70 μM) for 5 min. Cells were then washed, fixed with 4% paraformaldehyde, mounted on coverslips and analyzed by fluorescence

microscopy. For cells expressing BAP-TM, similar protocol was followed without the use of the antibody.

Targeting and Multimodal imaging of tumors with biotin-NLP-RPE *in vivo*. All animal studies were approved by the Subcommittee on Research Animal Care at Massachusetts General Hospital and were performed in accordance to their guidelines and regulations. Mice were kept on biotin-deficient diet throughout the study. One million Gli36 cells (in 50 µl) expressing BAP-TM or control cells were mixed with similar volume of Matrigel (Becton Dickinson) and implanted subcutaneously in the flanks of nude mice in 2 different locations. Two weeks later, mice (n=5) were injected with a complex of streptavidin-Alexa750 (200 µg) and biotin-NLP-RPE (200 µl of 7 mM) pre-incubated for 15 min. Mice were then imaged with fluorescence-mediated tomography and magnetic resonance at different time points.

Magnetic resonance imaging. MRI was performed using an animal 4.7 T MRI scanner (Bruker, Billerica, MA) consisting of coronal and axial T1w images (rapid acquisition with refocused echoes (RARE) sequence, TR=900 ms, TE=14.1 ms, field of view=5.4 cm x 4.0 cm, matrix size=256 x 256, slice thickness=1 mm, 16-18 slices) obtained before and after intravenous administration of Alexa750-SA-NLP-RPE or biotin-NLP-RPE as control as above. Post contrast images were obtained at 4 and 24 hrs post injection. Image analysis and segmentation was performed using the OsiriX™ DICOM viewer. Contrast-to-noise ratios were computed as (ROI_{tumor} – ROI_{muscle})/STD(noise), where ROI=region of interest drawn to encompass the tumor on the slice where the tumors are the largest or a region of flank muscle, and STD=standard deviation. For the 3D MRI image, the tumors were segmented out manually in the Amira environment (Visage Imaging, Inc., San Diego, CA). This was volume rendered in pseudocolor. The rest of the body was volume rendered in gray scale.

Fluorescence-mediated tomography. Quantitative fluorescent tomographic imaging was carried out on a commercial imaging system (FMT2500, Perkin Elmer, Waltham MA). Prior to imaging, mice received an intravenous injection of imaging agent. Four hours after injection, mice were non-invasively imaged under general

isoflurane anesthesia (1-1.5% at 2l/min). Paired absorption and fluorescent data sets were collected using a scanning laser, and 3-dimensional reconstructions were generated utilizing the TrueQuant FMT software.

ACKNOWLEDGEMENTS

This work was supported by grant from NIH/NCI 4R00CA126839 (BAT), and P50CA86355 (RW and BAT), as well as NIH/NINDS R01-NS070835 (JWC), R01-NS072167 (JWC), and P30NS045776 (BAT). The authors would like to thank Dr. Darell D. Bigner (Duke University Medical Center) for providing the antibody against EGFRvIII, Dr. Casey Maguire (MGH) for biotinylation of this antibody and Dr. Miguel Sena Esteves (Universisty of Massachusetts Medical Center) for providing the retrovirus vector expressing EGFRvIII.

REFERENCES

1. Weissleder R. (2002). Scaling down imaging: Molecular mapping of cancer in mice. *Nature Reviews Cancer.*2(1):11-18.
2. Hu FQ, Joshi HM, Dravid VP, Meade TJ. (2010). High-performance nanostructured MR contrast probes. *Nanoscale.*2(10):1884-1891.
3. Bae KH, Chung HJ, Park TG. (2011). Nanomaterials for cancer therapy and imaging. *Mol Cells.*31(4):295-302.
4. Barreto JA, O'Malley W, Kubeil M, Graham B, Stephan H, Spiccia L. (2011). Nanomaterials: applications in cancer imaging and therapy. *Adv Mater.*23(12):H18-40.
5. Mulder WJM, Strijkers GJ, Griffioen AW, van Bloois L, Molema G, Storm G, et al. (2004). A liposomal system for contrast-enhanced magnetic resonance imaging of molecular targets. *Bioconjugate Chemistry.*15(4):799-806.
6. Torchilin VP. (2005). Recent advances with liposomes as pharmaceutical carriers. *Nat Rev Drug Discov.*4(2):145-160.
7. Kozlowska D, Foran P, MacMahon P, Shelly MJ, Eustace S, O'Kennedy R. (2009). Molecular and magnetic resonance imaging: The value of immunoliposomes. *Adv Drug Deliv Rev.*61(15):1402-1411.
8. Mody VV, Nounou MI, Bikram M. (2009). Novel nanomedicine-based MRI contrast agents for gynecological malignancies. *Adv Drug Deliv Rev.*61(10):795-807.
9. Srikanth M, Kessler JA. (2012). Nanotechnology-novel therapeutics for CNS disorders. *Nat Rev Neurol.*8(6):307-318.
10. Kono K, Nakashima S, Kokuryo D, Aoki I, Shimomoto H, Aoshima S, et al. (2011). Multi-functional liposomes having temperature-triggered release and magnetic resonance imaging for tumor-specific chemotherapy. *Biomaterials.*32(5):1387-1395.
11. Shiraishi K, Kawano K, Minowa T, Maitani Y, Yokoyama M. (2009). Preparation and in vivo imaging of PEG-poly(L-lysine)-based polymeric micelle MRI contrast agents. *J Control Release.*136(1):14-20.
12. Fossheim SL, Il'yasov KA, Hennig J, Bjornerud A. (2000). Thermosensitive paramagnetic liposomes for temperature control during MR imaging-guided hyperthermia: in vitro feasibility studies. *Acad Radiol.*7(12):1107-1115.
13. Kielar F, Tei L, Terreno E, Botta M. (2010). Large relaxivity enhancement of paramagnetic lipid nanoparticles by restricting the local motions of the Gd(III) chelates. *J Am Chem Soc.*132(23):7836-7837.
14. Yatvin MB, Weinstein JN, Dennis WH, Blumenthal R. (1978). Design of liposomes for enhanced local release of drugs by hyperthermia. *Science.*202(4374):1290-1293.
15. de Smet M, Langereis S, van den Bosch S, Grull H. (2010). Temperature-sensitive liposomes for doxorubicin delivery under MRI guidance. *Journal of Controlled Release.*143(1):120-127.
16. Tagami T, Foltz WD, Ernsting MJ, Lee CM, Tannock IF, May JP, et al. (2011). MRI monitoring of intratumoral drug delivery and prediction of the therapeutic effect with a multifunctional thermosensitive liposome. *Biomaterials.*32(27):6570-6578.

17. Grull H, Langereis S. (2012). Hyperthermia-triggered drug delivery from temperature-sensitive liposomes using MRI-guided high intensity focused ultrasound. *J Control Release.*161(2):317-327.
18. Hak S, Sanders H, Agrawal P, Langereis S, Grull H, Keizer HM, et al. (2009). A high relaxivity Gd(III)DOTA-DSPE-based liposomal contrast agent for magnetic resonance imaging. *European Journal of Pharmaceutics and Biopharmaceutics.*72(2):397-404.
19. Peri S, Navarro JD, Amanchy R, Kristiansen TZ, Jonnalagadda CK, Surendranath V, et al. (2003). Development of human protein reference database as an initial platform for approaching systems biology in humans. *Genome Res.*13(10):2363-2371.
20. Tannous BA, Grimm J, Perry KF, Chen JW, Weissleder R, Breakefield XO. (2006). Metabolic biotinylation of cell surface receptors for in vivo imaging. *Nature Methods.*3(5):391-396.
21. Laurent S, Vander Elst L, Thirifays C, Muller RN. (2008). Relaxivities of paramagnetic liposomes: on the importance of the chain type and the length of the amphiphilic complex. *Eur Biophys J.*37(6):1007-1014.
22. Wang T, Hossann M, Reinl HM, Peller M, Eibl H, Reiser M, et al. (2008). In vitro characterization of phosphatidylglyceroglycerol-based thermosensitive liposomes with encapsulated 1H MR T1-shortening gadodiamide. *Contrast Media Mol Imaging.*3(1):19-26.
23. Koenig SH, Ahkong QF, Brown RD, 3rd, Lafleur M, Spiller M, Unger E, et al. (1992). Permeability of liposomal membranes to water: results from the magnetic field dependence of T1 of solvent protons in suspensions of vesicles with entrapped paramagnetic ions. *Magn Reson Med.*23(2):275-286.
24. Hak S, Sanders HM, Agrawal P, Langereis S, Grull H, Keizer HM, et al. (2009). A high relaxivity Gd(III)DOTA-DSPE-based liposomal contrast agent for magnetic resonance imaging. *Eur J Pharm Biopharm.*72(2):397-404.
25. van Dam GM, Themelis G, Crane LM, Harlaar NJ, Pleijhuis RG, Kelder W, et al. (2011). Intraoperative tumor-specific fluorescence imaging in ovarian cancer by folate receptor-alpha targeting: first in-human results. *Nat Med.*17(10):1315-1319.
26. Deliolanis NC, Dunham J, Wurdinger T, Figueiredo JL, Tannous BA, Ntziachristos V. (2009). In-vivo imaging of murine tumors using complete-angle projection fluorescence molecular tomography. *J Biomed Opt.*14(3):030509.
27. Axworthy DB, Reno JM, Hylarides MD, Mallett RW, Theodore LJ, Gustavson LM, et al. (2000). Cure of human carcinoma xenografts by a single dose of pretargeted yttrium-90 with negligible toxicity. *Proceedings of the National Academy of Sciences of the United States of America.*97(4):1802-1807.
28. Sakahara H, Saga T. (1999). Avidin-biotin system for delivery of diagnostic agents. *Advanced Drug Delivery Reviews.*37(1-3):89-101.
29. Hara T, Bhayana B, Thompson B, Kessinger CW, Khatri A, McCarthy JR, et al. (2012). Molecular imaging of fibrin deposition in deep vein thrombosis using fibrin-targeted near-infrared fluorescence. *JACC Cardiovasc Imaging.*5(6):607-615.
30. Yoo H, Kim JW, Shishkov M, Namati E, Morse T, Shubochkin R, et al. (2011). Intra-arterial catheter for simultaneous microstructural and molecular imaging in vivo. *Nat Med.*17(12):1680-1684.

31. Staruch R, Chopra R, Hynynen K. (2011). Localised drug release using MRI-controlled focused ultrasound hyperthermia. *Int J Hyperthermia.*27(2):156-171.
32. Carignan CS, Yagi Y. (2012). Optical endomicroscopy and the road to real-time, in vivo pathology: present and future. *Diagn Pathol.*7(1):98.
33. Rouser G, Fleische.S, Yamamoto A. (1970). 2 dimensional thin layer chromatographic separation of polar lipids and determination of phospholipids by phosphorus analysis of spots. *Lipids.*5(5):494-&.
34. Burtea CL, S.; Vander Elst, L.; and Muller, R. N. Contrast Agents: Magnetic Resonance. Molecular Imaging I, Handbook of Experimental Pharmacology. Vol 185(1):135-165. Springer Berlin Heidelberg; 2008.